JACS
JOURNAL OF THE AMERICAN CHEMICAL SOCIETY

Article

pubs.acs.org/JACS

# UV-Induced Proton-Coupled Electron Transfer in Cyclic DNA Miniduplexes

Yuyuan Zhang,[†] Xi-Bo Li,[‡] Aaron M. Fleming,[‡] Jordan Dood,[†,∥] Ashley A. Beckstead,[†] Anita M. Orendt,[‡,§] Cynthia J. Burrows,*[,‡] and Bern Kohler*[,†]

[†]Department of Chemistry and Biochemistry, Montana State University, Bozeman, Montana 59717, United States
[‡]Department of Chemistry, University of Utah, 315 S. 1400 East, Salt Lake City, Utah 84112, United States
[§]Center for High Performance Computing, University of Utah, Salt Lake City, Utah 84112-0190, United States

Supporting Information

**ABSTRACT:** The excited-state dynamics of two cyclic DNA miniduplexes, each containing just two base pairs, are investigated using time-resolved infrared spectroscopy. As in longer DNA duplexes, intrastrand electron transfer induced by UV excitation triggers interstrand proton transfer in the alternating miniduplex containing two out-of-phase G·C base pairs. The resulting excited state decays on a time scale of several tens of picoseconds. This state is absent when one of the two G residues is substituted by 8-oxo-7,8-dihydroguanine, a modification that is suggested to disrupt base stacking, while maintaining base pairing. These findings demonstrate that a nucleobase tetramer arranged as two stacked base pairs accurately captures the interplay between intrastrand and interstrand decay channels. The similar signals seen in the miniduplexes and longer sequences suggest that excited states in the latter rapidly localize on two adjacent base pairs.

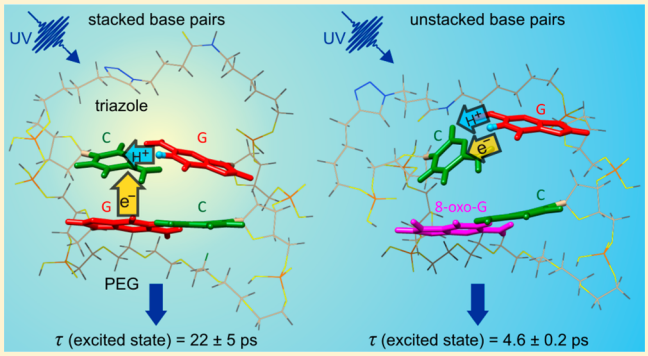


## INTRODUCTION

Recent time-resolved infrared (TRIR) pump−probe experiments reveal spectral and dynamical differences in UV excited states formed in double-stranded DNA duplexes containing 18 identical A·T base pairs, but differing in base sequence.[1] As in single-stranded DNA,[2−4] UV-excitation of DNA duplexes causes intrastrand electron transfer (ET) between adjacent bases on one strand, and can generate high yields of oppositely charged radical ions.[1,5] In certain sequences, interstrand proton transfer (PT) between a radical ion on one strand and its neutral complementary base on the opposite strand can additionally take place along a hydrogen bond (H-bond) and the overall excited-state mechanism is an example of photo-induced proton-coupled electron transfer (PCET).[1,5] The enhanced acidity/basicity of the ions compared to their neutral parent molecules (see Table S1 in ref 1, and ref 6) is the driving force behind interstrand PT. Photoinduced PCET explains why attempts to reduce excited-state dynamics in DNA duplexes to pairwise interactions between bases that are *only* $\pi$-stacked or H-bonded fail to capture the full spectrum of photophysical pathways. Four bases arranged as two stacked base pairs thus appear to constitute a minimal model system for understanding excited-state dynamics in double-stranded DNA.

To test this paradigm, we report here a study of the excited-state dynamics of two cyclic DNA miniduplexes by TRIR spectroscopy. These structures, which contain just two base pairs, are the smallest systems that can support the PCET mechanism discussed in refs 1 and 5. At the same time, their small size will allow detailed study by high-level quantum chemical calculations. We show that the transient species generated in a miniduplex are identical to ones seen in a longer sequence containing 18 base pairs. The results strengthen the evidence that PCET is a general decay pathway in duplex DNA and suggest that excited states delocalized over more than two base pairs are not present in the alternating duplex made of 18 G·C base pairs on the time scale of the experiments ($t$ > 200 fs).

## RESULTS AND DISCUSSION

The two miniduplexes are cyclized oligonucleotides prepared from hairpin conjugates that contain a hexaethylene glycol (PEG) linker, a 5′-alkyne, and a 3′-azide. The latter two groups are converted to a triazole via Cu(I)-catalyzed click chemistry (see the Supporting Information, SI).[7,8] The PEG linker lacks double bonds and does not absorb photons with wavelengths longer than 200 nm.[9] The triazole linker exhibits an absorption band at 210 nm but cannot be excited significantly at 265 nm (see Figure S1 in the SI), the excitation wavelength in our TRIR experiments (full experimental details are described in

**Received:** March 29, 2016
**Published:** May 20, 2016





DOI: 10.1021/jacs.6b03216
J. Am. Chem. Soc. 2016, 138, 7395−7401

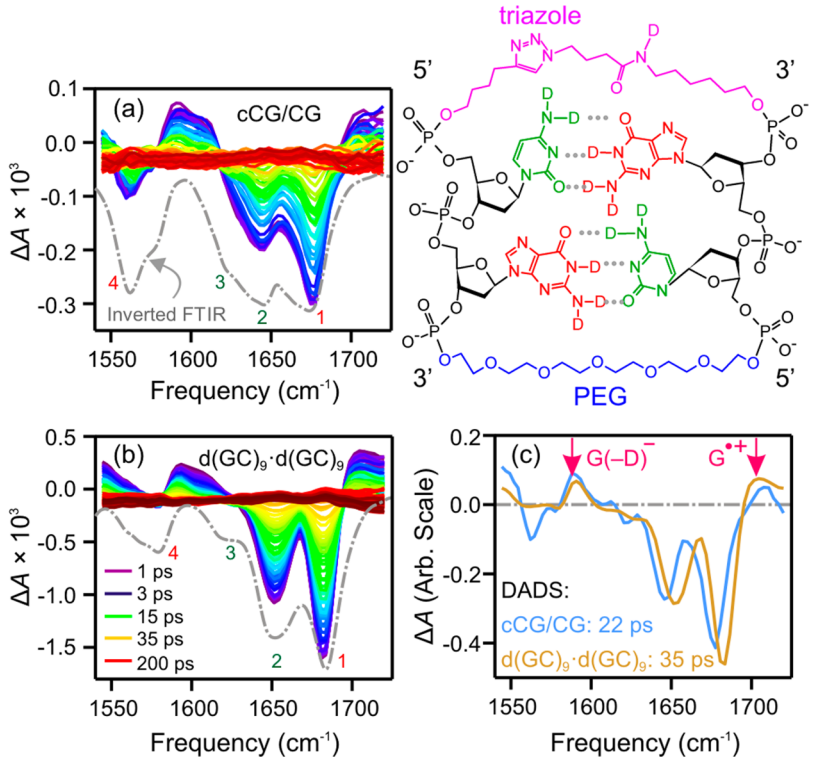


**Figure 1.** TRIR spectra recorded from 1 ps (purple) to 800 ps (red) after 265 nm excitation of (a) cCG/CG (structure shown on the right) and (b) $d(GC)_9 \cdot d(GC)_9$ in $D_2O$ solution with 50 mM $D_2PO_4^-$/ $DPO_4^{2-}$ buffer and 100 mM NaCl. The same color scale is used in panels (a) and (b). The inverted FTIR spectra are shown by the gray dash-dotted lines. (c) Decay-associated difference spectra (DADS) of the long-lived excited states of the two duplexes obtained from global fitting (see text). The two curves were scaled to have approximately equal intensity.

the SI). Exciton-coupled circular dichroism (ECCD, Figures S2 and S3) and nuclear magnetic resonance (NMR, Figure S4) measurements suggest that the cyclic miniduplex with two G·C base pairs (denoted cCG/CG, structure shown in Figure 1) adopts a stable B-form conformation at room temperature like the similar cGC/GC cyclic miniduplex reported by Brown and co-workers.[7]

Comparing the ground-state IR absorption spectra (the inverted FTIR spectra are shown by dash-dotted lines in panels (a) and (b) of Figure 1) reveals structural similarities and differences between cCG/CG and $d(GC)_9 \cdot d(GC)_9$. The latter, containing nine times as many G·C base pairs as the former, is expected to have few, if any, unstacked/unpaired bases. The FTIR spectrum of B-form $d(GC)_9 \cdot d(GC)_9$ shows a sharper carbonyl stretching mode of guanine ($G_{C=O}$, band 1) at ~1675 $cm^{-1}$ compared to cCG/CG. The broader $G_{C=O}$ band seen in cCG/CG may be due to a guanine that is not base paired with cytosine because the $G_{C=O}$ of the G monomer occurs at ~1665 $cm^{-1}$.[10] Additionally, the shoulder (band 3) at the low frequency side of the ~1650 $cm^{-1}$ band (band 2, assigned to the C=O stretching mode of cytosine, $C_{C=O}$) is less intense in $d(GC)_9 \cdot d(GC)_9$. This shoulder has reduced intensity when poly(dC) is based paired with poly(dG).[11] Lastly, the ring in-plane stretching mode of guanine (band 4, $G_{ring}$) at ~1575 $cm^{-1}$ is much weaker in $d(GC)_9 \cdot d(GC)_9$. The reduced intensity of the $G_{ring}$ mode has been interpreted as a hallmark of G·C base pairing.[11] Thus, the FTIR spectra suggest that not all bases in the cyclic miniduplex cCG/CG are stably base paired as in $d(GC)_9 \cdot d(GC)_9$. Imperfect base pairing has been reported previously for a hairpin containing two G·C base pairs linked by a PEG group.[12] It is difficult, however, to determine the fraction of the unpaired bases in cCG/CG using the current steady-state data.[13]

The instrumentation for recording TRIR spectra is described in ref 14 and experimental details are given in the SI. The TRIR spectra in the double-bond stretching region for cCG/CG and $d(GC)_9 \cdot d(GC)_9$ in buffered $D_2O$ solution, collected from 1 to 800 ps after 265 nm excitation, are displayed in panels (a) and (b) of Figure 1. Negative peaks align well with minima in the inverted FTIR spectra and are assigned to ground state bleach (GSB) signals. Weak positive signals due to excited-state absorption (ESA) or absorption by transient species are also observed at 1550, 1600, and 1700 $cm^{-1}$. The TRIR signal of the miniduplex is much weaker than that of the $d(GC)_9 \cdot d(GC)_9$ duplex due to the lower concentration of the former and the pump pulse energies used. Importantly, the pump pulse fluences are low enough in all experiments that the probability of having more than one excitation in a single duplex is negligible (see the SI for details).

Global fitting of the TRIR data in the spectral and temporal domains[15] was performed using the Glotaran software package (see the SI for details).[16] The fits show that the positive and negative signals decay biexponentially with time constants of 5.0 ± 0.7 and 22 ± 5 ps for cCG/CG, and 7.2 ± 0.5 and 35 ± 2 ps for $d(GC)_9 \cdot d(GC)_9$. The decay constants obtained for $d(GC)_9 \cdot d(GC)_9$ are in excellent agreement with previous reports.[1,5,17] Figure 2 shows the kinetic trace of the strongest GSB signal and its fit obtained from global analysis. All signals decay to a featureless negative offset across the probing region, which is due to laser-induced heating of $D_2O$.[18]

Differences with the FTIR spectra of the two duplexes are evident in the early time TRIR spectra (1–20 ps after excitation), and will be discussed later. The amplitude of the


DOI: 10.1021/jacs.6b03216
J. Am. Chem. Soc. 2016, 138, 7395–7401

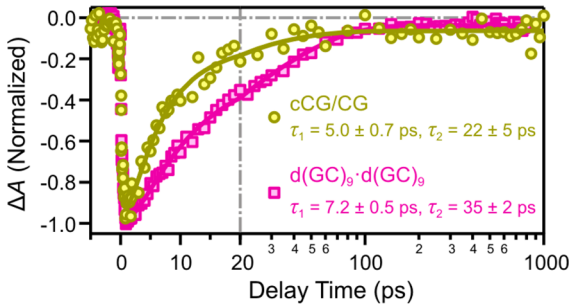


**Figure 2.** Ground-state bleach recovery of $G_{C=O}$ (band 1 in Figure 1) for cCG/CG (olive green) and $d(GC)_9 \cdot d(GC)_9$ (magenta). The markers are the experimental TRIR signals and solid lines are global fits. The vertical dash-dotted line designates the linear-logarithmic break in the horizontal axis.

long-lived component is greatly reduced in cCG/CG compared to $d(GC)_9 \cdot d(GC)_9$, as seen in Figure 2 (approximately 15 ± 8% of the total amplitude for cCG/CG vs 60 ± 5% for $d(GC)_9 \cdot d(GC)_9$). We propose that this is due to the presence of a greater number of conformers in the miniduplex, which cannot undergo the photoinduced PCET mechanism indicated in Figure 3, possibly because of poor base stacking and/or base pairing. Strikingly, despite the differences in the early time TRIR spectra and the relative amplitudes of the fast and slow decay components (see Figure S5 and the associated text in the SI with global fitting details), the long-lived spectra of the two duplexes are very similar (Figure 1c). The small shift in the major GSB bands (bands 1 and 2) may be due to minor structural differences between cCG/CG and $d(GC)_9 \cdot d(GC)_9$. The positions of vibrational bands in the double-bond stretching region are exquisitely sensitive to conformation as is evident from the significant differences seen in the FTIR spectra of B- and Z-forms of the alternating G·C duplex.[17] Importantly, the C=O stretching modes (bands 1 and 2) in the cCG/CG long-lived spectra are considerably narrower than those observed in the FTIR spectrum, and are as sharp as the features seen in $d(GC)_9 \cdot d(GC)_9$. This indicates that only the stacked and paired bases undergo slow excited-state relaxation.

The spectral signatures of $G^{\bullet+}$ and $G(-D1)^-$ are clearly observed in both duplexes. The $C(+D3)^{\bullet}$ vibrational marker band is predicted to appear at approximately 1625 $cm^{-1}$, masking the GSB of band 3.[1,5] These transient species can only be generated by the PCET mechanism indicated in Figure 3, where both electron and proton move from two different guanine residues toward a cytosine residue, forming a distonic radical ion base pair $C(+D3)^{\bullet} \cdot G(-D1)^-$ stacked with a nondistonic $G^{\bullet+} \cdot C$ base pair. The similar long-lived excited-state spectra indicate that identical transient species are formed in UV-excited cCG/CG and $d(GC)_9 \cdot d(GC)_9$. The observation of the closed-shell ion $G(-D1)^-$ is the key evidence supporting our model. This transient species is not observed in the Hoogsteen form of the $d(GC)_9 \cdot d(GC)_9$ duplex, which lacks the N1−D···N3 H-bond.[5]

We next consider possible explanations for the longer lifetime (35 ± 2 ps) observed for $d(GC)_9 \cdot d(GC)_9$ compared to cCG/CG (22 ± 5 ps). The common excited state formed in each is proposed to decay when the electron and proton return to their original positions. This can take place concertedly, but recent experiments on Watson−Crick and Hoogsteen $d(GC)_9 \cdot d(GC)_9$ duplexes suggest that back ET occurs first, followed by ultrafast PT.[5] Charge delocalization, charge transport, or solvation differences could affect back ET rates in both systems. We consider these possibilities in order in the following paragraphs.

A longer strand with three or more base pairs can support charge delocalization over more than two base pairs[3,19] or even charge transport.[20] In this case, the longer excited-state decay time observed in $d(GC)_9 \cdot d(GC)_9$ would reflect slower recombination of delocalized charges and/or free charges that are several bases apart. However, charge delocalization, even in single DNA strands, is a controversial issue. Bucher et al. concluded from their TRIR experiments that the charge generated by intrastrand ET extends over as many as four uracil bases.[3] On the other hand, Su et al. argued that electronic excitation is localized on no more than two bases in $d(A)_n$ sequences[21] in agreement with the conclusions of some computational studies.[22,23] Although charge-transfer states are predicted to delocalize over several bases in nonalternating sequences, alternating sequences are less prone to delocalization effects due to the energy mismatch between the lowest excited states of neighboring bases that are not identical.[24,25]

Charge transport—the process in which an electron or hole moves relatively freely along a DNA strand—can occur when an initially bound electron−hole pair dissociates into free

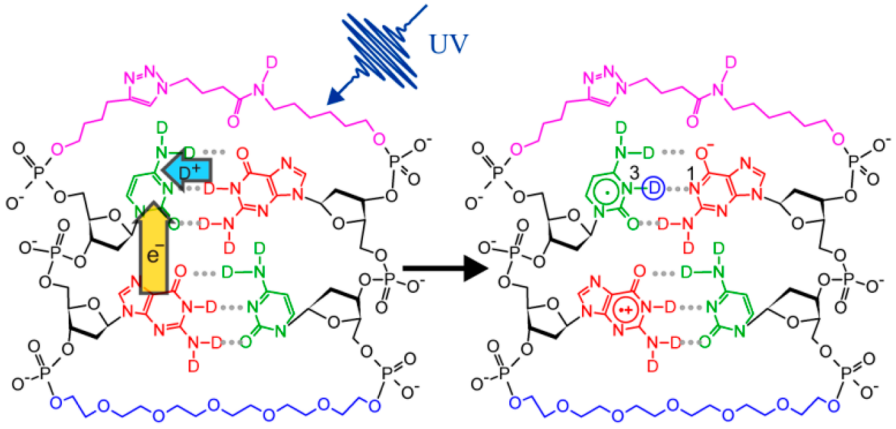


**Figure 3.** UV-induced proton-coupled electron transfer (PCET) resulting from intrastrand electron transfer (ET) and interstrand proton transfer (PT) in cCG/CG. In $D_2O$ solution, a deuteron (colored blue at right) moves toward the electron, yielding a distonic radical ion base pair in the upper base pair.



DOI: 10.1021/jacs.6b03216
J. Am. Chem. Soc. 2016, 138, 7395−7401

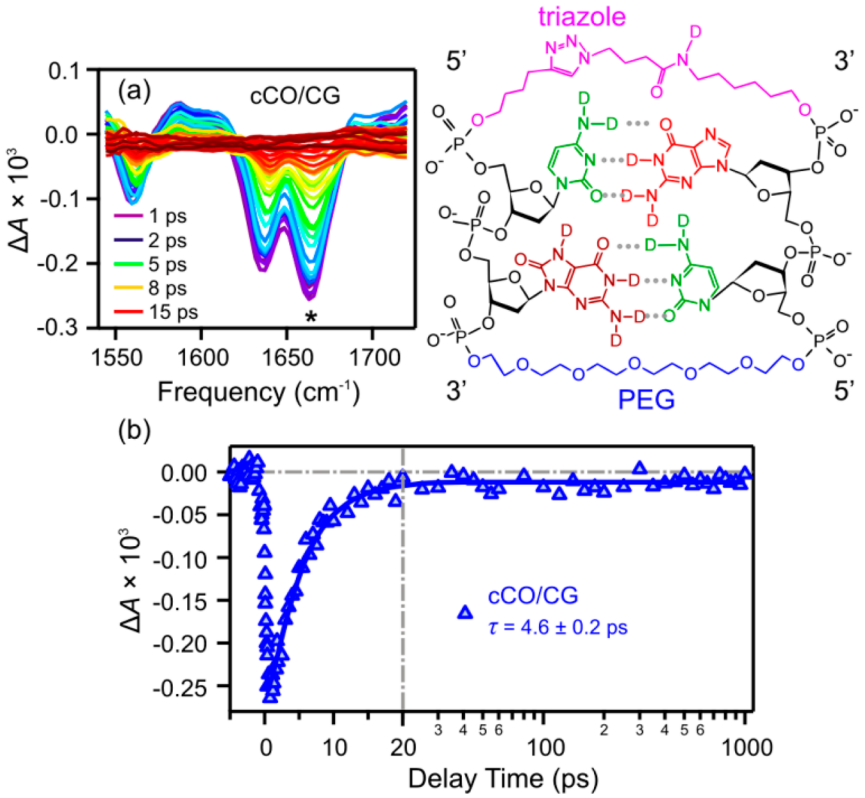


**Figure 4.** (a) TRIR spectra recorded between 1 ps (purple) and 50 ps (red) after 265 nm excitation of cCO/CG (structure shown on the right) in $D_2O$ solution with 50 mM $D_2PO_4^-$/ $DPO_4^{2-}$ buffer and 100 mM NaCl. (b) Ground-state bleach (GSB) recovery monitored at 1662 $cm^{-1}$ (frequency indicated by an asterisk in panel a). The markers are the experimental TRIR signals, the solid curve is from a global fit. The vertical dash-dotted line designates the linear-logarithmic break.

charges. This requires that electron and hole overcome ~0.5 eV of Coulomb attraction[26] and increase their separation by moving to more distant base pairs. This is impossible in cCG/CG, but could take place in the longer $d(GC)_9{\cdot}d(GC)_9$. Charge delocalization has been suggested to facilitate the dissociation of a bound electron−hole pair,[27] but it should be strongly inhibited in a domain of alternating bases for the reasons just mentioned.

The unlikelihood of charge delocalization or charge transport suggests that excited states in $d(GC)_9{\cdot}d(GC)_9$ involve two adjacent base pairs just like the ones in cCG/CG. The similar nature of excited states in both systems provides the simplest explanation for the common TRIR spectra observed in both duplexes. Calculations seeking to explain excited states with unusually high emission energies and nanosecond lifetimes in an alternating GC duplex recently identified mixed Frenkel exciton/charge transfer states that are largely limited to two base pairs.[28] Although there is no evidence in our measurements of excited states with nanosecond lifetimes, possibly because such states are formed in very low quantum yield, this study does reinforce the viewpoint that excited states with significant charge transfer character are strongly localized in alternating sequences. Charge delocalization could still take place in other DNA sequences, especially ones with domains of identical bases, but definitive evidence is lacking. Variable-length, nonalternating G·C miniduplexes containing two or more base pairs could be useful model systems for searching for evidence of delocalization.

We propose that the faster decay seen for the cCG/CG miniduplex vs $d(GC)_9{\cdot}d(GC)_9$ is due to their very different solvation environments. In the miniduplex, all four bases are exposed to water to a substantial degree, while excited-state dynamics in the 18-mer double strand is dominated by contributions from base tetramers in the interior. It has been shown that semiclassical nonadiabatic Marcus theory can successfully model back ET rates in single-stranded DNA.[29] The reorganization energy for charge recombination is expected to be lower for the $d(GC)_9{\cdot}d(GC)_9$ duplex compared to the cCG/CG miniduplex due to the reduced dielectric constant experienced by interior bases in the longer system. Because back ET takes place in the Marcus-inverted region[29] increasing reorganization energy correlates with increased back ET rates, assuming that the thermodynamic driving force and electronic coupling remain constant. Thus, the greater reorganization energy expected for the more hydrated base pairs in cCG/CG results in a higher rate of decay in agreement with the observed trend in lifetimes.

We replaced one of the guanine residues in the cCG/CG miniduplex by 8-oxo-7,8-dihydroguanine (8-oxo-G). The resulting miniduplex, denoted cCO/CG (see structure in Figure 4), contains one G·C and one O·C base pair. Figure 4a presents the TRIR spectra of cCO/CG in buffered $D_2O$ solution recorded between 1 and 50 ps following 265 nm excitation. The TRIR signals disappear by approximately 20 ps, leaving a constant offset across the spectral region due to $D_2O$ heating as discussed above. Global fitting reveals a mono-exponential decay with a time constant of 4.6 ± 0.2 ps.

The elimination of the long-lived decay component seen in cCG/CG upon modification of a single G is surprising at first glance. Because O is a better electron donor than G,[30,31]


DOI: 10.1021/jacs.6b03216
J. Am. Chem. Soc. 2016, 138, 7395−7401

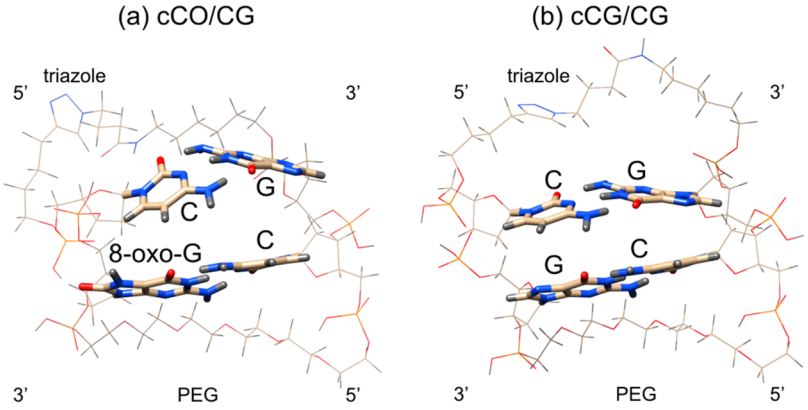


**Figure 5.** Optimized structures for (a) cCO/CG and (b) cCG/CG at the B3LYP/6-311G(d,) level. Images were prepared using the UCSF Chimera software package.[36]

intrastrand ET should be facile in CpO. The resulting $C^{\bullet-}$, stacked with $O^{\bullet+}$, should acquire a deuteron from its H-bonded partner G along the middle H-bond, forming the same distonic radical ion base pair $G(-D1)^{-}\cdot C(+D3)^{\bullet}$ as in cGC/CG (the top base pair shown on the right side of Figure 3). G → C ET on the opposite strand would also be followed by PT from N1 of O to N3 of $C^{\bullet-}$ in the resulting $O\cdot C^{\bullet-}$ base pair. This follows because O is a better acid than G (the $pK_a$ values for G/$G(-H1)^{-}$ and O/$O(-H1)^{-}$ are 9.4[32] and 8.6,[33] respectively). In both scenarios, a longer decay component is expected.

The absence of a long-lived decay component in cCO/CG is suggested to arise from poor base stacking. Although the two miniduplexes differ only by the substituents on two atoms of a single G residue, evidence points to significant structural differences. The O·C base pair is expected to have the same Watson−Crick H-bonding motif as the G·C base pair,[34] and NMR spectroscopy indicates that both G·C and O·C are properly base paired (Figure S4). However, the two base pairs are poorly stacked in the calculated structure of cCO/CG (Figure 5a) that best reproduces the ECCD spectrum (Figure S3); the internucleotide distances (defined as the distance between the C5 atoms) are 5.13 and 6.56 Å for CpO and CpG, respectively. These distances are much greater than the average distance between $\pi$-stacked C and G in cCG/CG of 3.86 Å (Figure 5b). Structural studies have previously identified a steric clash between the C8 carbonyl of 8-oxo-G and the O4 and the 5′-phosphate oxygen of the same nucleotide, which is relieved by a minor change in bond angles.[35] In the case of the cCO/CG miniduplex, the 5′ phosphate closest to the triazole reorients, causing the G·C base pair to buckle in the DFT-optimized structure (Figure 5a). The greater separation between base pairs in cCO/CG provide an unusual opportunity to observe the effects of base pairing on excited-state dynamics in the absence of well-ordered base stacking in aqueous solution.

We propose that the 4.6 ps component seen in cCO/CG reflects relaxation taking place within single base pairs in the miniduplex. In a landmark computational study, it was shown that excitation of an isolated G·C base pair transfers an electron and a proton from G to C followed by decay to the ground state via an $S_1/S_0$ conical intersection (CI).[37] The overall mechanism of electron-driven proton transfer was subsequently described for an isolated A·T base pair.[38] Broad spectral lines consistent with short excited-state lifetimes were observed in spectroscopic experiments on single G·C base pairs in the gas phase,[39] but the decay kinetics were not observable. A recent computational study by Kumar and Sevilla suggests that the same mechanism is operative in the isolated O·C base pair.[40] Because all three bases in cCO/CG can absorb at the pump wavelength, the 4.6 ps component could reflect deactivation occurring in both base pairs on similar time scales.

Very recently, the biradical state produced by the transfer of an H atom (an electron-driven PT mechanism as described above) from G to C along the middle H-bond of single G·C base pairs was detected in chloroform solution.[41] This biradical state formed by interstrand H atom transfer was observed to decay with a lifetime of 2.9 ps.[41] The short lifetime is largely harmonious with theoretical predictions,[37] even if relaxation takes place somewhat more slowly than might have been expected for a barrierless process. Bleach recovery signals in ref 41 decay with a lifetime of 7.2 ps due to vibrational cooling. This lifetime, which was measured in chloroform solution, is similar to the 4.6 ps lifetime measured here in aqueous solution. In general, vibrational cooling takes place more rapidly in aqueous solution compared to other solvents.[42]

The TRIR spectra recorded between 1 and 5 ps do not exhibit the 'rise, blue-shift, and decay' dynamics that are the typical signature of VC on the ground state.[14] This could indicate that the lifetime of a biradical state is closer to the 4.6 ps lifetime as slower IC will wash out the contribution to the bleach recovery signals from VC. The lack of a VC signature may also indicate that all bases in cCO/CG are located in stable base pairs. An excited state of any base that is neither stacked nor base paired would be expected to decay on a subpicosecond time scale, resulting in VC on the ground electronic state. In addition, the TRIR spectrum of the C monomer exhibits a strong positive signature at ∼1570 $cm^{-1}$ with a lifetime of ∼30 ps.[43] The absence of these signatures suggests that monomer-like decay is not an important pathway.

Definitive assignment of the 4.6 ps state is not possible at this time also because the observed dynamics are likely a composite of interstrand H atom transfer in both the G·C and O·C base pairs. Preliminary calculations performed on the neutral 9-methyl-$G(-D1)^{\bullet}$ radical H-bonded with the neutral 1-methyl-$C(+D3)^{\bullet}$ radical predicts a positive feature at approximately 1630 $cm^{-1}$ (see Figure S6 in ref 1[45]). In comparison, positive signals are observed in the 1580−1620 $cm^{-1}$ region (Figure 4a) not far from the predicted position. Analogous calculations for vibrational modes of an O·C base pair have not yet been reported.

The excited-state dynamics in these two closely related miniduplexes richly illustrate the competition between


DOI: 10.1021/jacs.6b03216
J. Am. Chem. Soc. 2016, 138, 7395−7401

interstrand electron-driven PT[37,38] and the PCET mechanism first described in ref 1. Evidence suggests that both channels are accessible even when all bases are stacked and paired.[9] In the absence of base stacking, interstrand electron-driven PT, which results in ultrafast IC to the electronic ground state, is the only operative channel, while intrastrand ET[44] (and the interstrand PT coupled to it)[1] can only be observed when stacked bases are present. Interestingly, radicals formed on the same strand via intrastrand ET (and possibly followed by interstrand PT) are much longer-lived than ones formed by electron-driven PT in poorly stacked base pairs. The long lifetimes observed in the former case are due to charge recombination that takes place deep in the Marcus-inverted region.[29]

The competition between the two channels in regular duplexes containing stacked base pairs appears to be strongly influenced by energetics. When C is stacked with G, the intrastrand ET channel lies lower in energy compared to interstrand ET.[25] On the other hand, in sequences with repeating nucleotides (i.e., ApA, GpG, CpC, TpT) interstrand ET may be more accessible than intrastrand ET on account of the lower driving force for charge separation between identical nucleobases.[24,25] Consistent with this hypothesis, the amplitude of the faster decay component that is assigned to electron-driven PT in base pairs is larger in duplexes with nonalternating vs alternating base sequence.[1]

## CONCLUSIONS

We have observed the excited-state dynamics by TRIR spectroscopy of the shortest possible DNA duplex that possesses both base stacking and pairing. The photophysical pathways in cCG/CG are remarkably similar to those in the longer $d(GC)_9 \cdot d(GC)_9$ duplex, suggesting that excited states in the latter system are localized over just two base pairs. In sequences where intrastrand ET is more favorable than interstrand ET (e.g., in cCG/CG and $d(GC)_9 \cdot d(GC)_9$), charge separation between two $\pi$-stacked nucleobases on the same strand leads to a pair of radical ions, which can trigger interstrand PT, even in a duplex containing just two base pairs. The state reached by intrastrand ET and interstrand PT subsequently decays on a time scale of tens to hundreds of picoseconds. In contrast, in sequences with more easily accessible interstrand ET (e.g., cCO/CG and nonalternating duplexes), short-lived excited states are proposed to be more prominent due to rapid IC by interstrand electron-driven PT, which constitutes an additional PCET decay channel.

The ability to incorporate modified nucleobases, such as 8-oxoguanine, into cyclic miniduplexes offers a route to selective excitation and probing of specific residues. Replacing a single G by 8-oxo-G in the cCG/CG miniduplex greatly accelerates excited-state relaxation. Although further structural characterization of the cCO/CG miniduplex is needed, this system appears to have well-formed base pairs that are nevertheless poorly stacked and possibly separated by water molecules. These observations support for the first time in aqueous solution the electron-driven PT deactivation channel predicted for the isolated G·C base pair.[37] They also illustrate the exquisite sensitivity of excited-state deactivation in duplex DNA to the interplay between intrastrand and interstrand processes.

## ASSOCIATED CONTENT

### Supporting Information

The Supporting Information is available free of charge on the ACS Publications website at DOI: 10.1021/jacs.6b03216.

Synthesis, characterization, DFT geometric optimization coordinates and energies, TD-DFT spectra of the miniduplexes, UV−visible spectrum of triazole, and TRIR experimental methods (PDF)

## AUTHOR INFORMATION


### Corresponding Authors

*bkohler@montana.edu

*burrows@chem.utah.edu

### Present Address

[‖]J.D.: School of Medicine and Biomedical Sciences, The University at Buffalo, SUNY, Buffalo, NY 14214.


### Notes

The authors declare no competing financial interest.

## ACKNOWLEDGMENTS

Work at Montana State University was supported by NSF (CHE-1465277). The TRIR spectrometer was constructed with funding from the M. J. Murdock Charitable Trust. Work at University of Utah was supported by NSF (CHE-1507813). A.M.O. is supported in part by a National Science Foundation grant (1341935). Computational resources are gratefully acknowledged from the Center for High Performance Computing at the University of Utah.

## REFERENCES


(1) Zhang, Y.; de La Harpe, K.; Beckstead, A. A.; Improta, R.; Kohler, B. *J. Am. Chem. Soc.* **2015**, *137*, 7059.

(2) Doorley, G. W.; Wojdyla, M.; Watson, G. W.; Towrie, M.; Parker, A. W.; Kelly, J. M.; Quinn, S. J. *J. Phys. Chem. Lett.* **2013**, *4*, 2739.

(3) Bucher, D. B.; Pilles, B. M.; Carell, T.; Zinth, W. *Proc. Natl. Acad. Sci. U. S. A.* **2014**, *111*, 4369.

(4) Zhang, Y.; Dood, J.; Beckstead, A. A.; Li, X.-B.; Nguyen, K. V.; Burrows, C. J.; Improta, R.; Kohler, B. *Proc. Natl. Acad. Sci. U. S. A.* **2014**, *111*, 11612.

(5) Zhang, Y.; de La Harpe, K.; Beckstead, A. A.; Martínez-Fernández, L.; Improta, R.; Kohler, B. *J. Phys. Chem. Lett.* **2016**, *7*, 950.

(6) Kumar, A.; Sevilla, M. D. *Chem. Rev.* **2010**, *110*, 7002.

(7) El-Sagheer, A. H.; Kumar, R.; Findlow, S.; Werner, J. M.; Lane, A. N.; Brown, T. *ChemBioChem* **2008**, *9*, 50.

(8) El-Sagheer, A. H.; Brown, T. *Acc. Chem. Res.* **2012**, *45*, 1258.

(9) Chen, J.; Thazhathveetil, A. K.; Lewis, F. D.; Kohler, B. *J. Am. Chem. Soc.* **2013**, *135*, 10290.

(10) Banyay, M.; Sarkar, M.; Gräslund, A. *Biophys. Chem.* **2003**, *104*, 477.

(11) Liquier, J.; Taillandier, E. In *Infrared Spectroscopy of Biomolecules*; Mantsch, H. H., Chapman, D., Eds.; Wiley-Liss, Inc.: New York, 1996; p 131.

(12) Brazard, J.; Thazhathveetil, A. K.; Vaya, I.; Lewis, F. D.; Gustavsson, T.; Markovitsi, D. *Photochem. Photobiol. Sci.* **2013**, *12*, 1453.

(13) To estimate the fraction of the unpaired bases in cCG/CG, we used a linear combination of FTIR spectra of dGMP, dCMP, and $d(GC)_9 \cdot d(GC)_9$ to model the FTIR spectrum of cCG/CG. This approach failed because single-stranded $d(GC)_9$, representing the stacked but unpaired fraction, is also needed. However, it is impossible to obtain this FTIR spectrum due to the fact that $d(GC)_9$ is self-complementary. Using melting data from UV−vis, ECCD, or NMR spectroscopy to estimate the unpaired fraction is also difficult, because cCG/CG does not have enough base pairs to exhibit a clear melting transition as normally observed in the cooperative melting of multiple base pairs.

(14) Zhang, Y.; Chen, J.; Kohler, B. *J. Phys. Chem. A* **2013**, *117*, 6771.

(15) van Stokkum, I. H. M.; Larsen, D. S.; van Grondelle, R. *Biochim. Biophys. Acta, Bioenerg.* **2004**, *1657*, 82.




DOI: 10.1021/jacs.6b03216
J. Am. Chem. Soc. 2016, 138, 7395−7401

(16) Snellenburg, J. J.; Laptenok, S. P.; Seger, R.; Mullen, K. M.; van Stokkum, I. H. M. *J. Stat. Softw.* **2012**, *49*, 1.
(17) Doorley, G. W.; McGovern, D. A.; George, M. W.; Towrie, M.; Parker, A. W.; Kelly, J. M.; Quinn, S. J. *Angew. Chem., Int. Ed.* **2009**, *48*, 123.
(18) Schreier, W. J.; Schrader, T. E.; Koller, F. O.; Gilch, P.; Crespo-Hernández, C. E.; Swaminathan, V. N.; Carell, T.; Zinth, W.; Kohler, B. *Science* **2007**, *315*, 625.
(19) Conwell, E. M.; McLaughlin, P. M.; Bloch, S. M. *J. Phys. Chem. B* **2008**, *112*, 2268.
(20) Genereux, J. C.; Barton, J. K. *Chem. Rev.* **2010**, *110*, 1642.
(21) Su, C.; Middleton, C. T.; Kohler, B. *J. Phys. Chem. B* **2012**, *116*, 10266.
(22) Plasser, F.; Aquino, A. J. A.; Hase, W. L.; Lischka, H. *J. Phys. Chem. A* **2012**, *116*, 11151.
(23) Improta, R.; Barone, V. *Angew. Chem., Int. Ed.* **2011**, *50*, 12016.
(24) Lange, A. W.; Herbert, J. M. *J. Am. Chem. Soc.* **2009**, *131*, 3913.
(25) Ko, C.; Hammes-Schiffer, S. *J. Phys. Chem. Lett.* **2013**, *4*, 2540.
(26) Olaso-González, G.; Roca-Sanjuán, D.; Serrano-Andrés, L.; Merchán, M. *J. Chem. Phys.* **2006**, *125*, 231102.
(27) Bakulin, A. A.; Rao, A.; Pavelyev, V. G.; van Loosdrecht, P. H. M.; Pshenichnikov, M. S.; Niedzialek, D.; Cornil, J.; Beljonne, D.; Friend, R. H. *Science* **2012**, *335*, 1340.
(28) Huix-Rotllant, M.; Brazard, J.; Improta, R.; Burghardt, I.; Markovitsi, D. *J. Phys. Chem. Lett.* **2015**, *6*, 2247.
(29) Zhang, Y.; Dood, J.; Beckstead, A. A.; Li, X.-B.; Nguyen, K. V.; Burrows, C. J.; Improta, R.; Kohler, B. *J. Phys. Chem. B* **2015**, *119*, 7491.
(30) Steenken, S.; Jovanovic, S. V.; Bietti, M.; Bernhard, K. *J. Am. Chem. Soc.* **2000**, *122*, 2373.
(31) Psciuk, B. T.; Schlegel, H. B. *J. Phys. Chem. B* **2013**, *117*, 9518.
(32) Ts'o, P. O. P. In *Basic Principles in Nucleic Acid Chemistry*; Ts'o, P. O. P., Ed.; Academic Press: New York, 1974; p 454−584.
(33) Culp, S. J.; Cho, B. P.; Kadlubar, F. F.; Evans, F. E. *Chem. Res. Toxicol.* **1989**, *2*, 416.
(34) Nguyen, K. V.; Burrows, C. J. *J. Am. Chem. Soc.* **2011**, *133*, 14586.
(35) Lipscomb, L. A.; Peek, M. E.; Morningstar, M. L.; Verghis, S. M.; Miller, E. M.; Rich, A.; Essigmann, J. M.; Williams, L. D. *Proc. Natl. Acad. Sci. U. S. A.* **1995**, *92*, 719.
(36) Pettersen, E. F.; Goddard, T. D.; Huang, C. C.; Couch, G. S.; Greenblatt, D. M.; Meng, E. C.; Ferrin, T. E. *J. Comput. Chem.* **2004**, *25*, 1605.
(37) Sobolewski, A. L.; Domcke, W. *Phys. Chem. Chem. Phys.* **2004**, *6*, 2763.
(38) Perun, S.; Sobolewski, A. L.; Domcke, W. *J. Phys. Chem. A* **2006**, *110*, 9031.
(39) Abo-Riziq, A.; Grace, L.; Nir, E.; Kabelac, M.; Hobza, P.; de Vries, M. S. *Proc. Natl. Acad. Sci. U. S. A.* **2005**, *102*, 20.
(40) Kumar, A.; Sevilla, M. D. *Photochem. Photobiol. Sci.* **2013**, *12*, 1328.
(41) Röttger, K.; Marroux, H. J. B.; Grubb, M. P.; Coulter, P. M.; Böhnke, H.; Henderson, A. S.; Galan, M. C.; Temps, F.; Orr-Ewing, A. J.; Roberts, G. M. *Angew. Chem., Int. Ed.* **2015**, *54*, 14719.
(42) Middleton, C. T.; Cohen, B.; Kohler, B. *J. Phys. Chem. A* **2007**, *111*, 10460.
(43) Quinn, S.; Doorley, G. W.; Watson, G. W.; Cowan, A. J.; George, M. W.; Parker, A. W.; Ronayne, K. L.; Towrie, M.; Kelly, J. M. *Chem. Commun.* **2007**, 2130.
(44) Chen, J.; Zhang, Y.; Kohler, B. *Top. Curr. Chem.* **2014**, *356*, 39.
(45) Incorrect atom numbers were used in the description of panel D of Figure S6 in ref 1. The species shown is 9me-G(−D1)$^{\bullet}$·1me-C(+D3)$^{\bullet}$.



DOI: 10.1021/jacs.6b03216
*J. Am. Chem. Soc.* 2016, 138, 7395−7401